Available online at www.sciencedirect.com
ScienceDirect
Journal of Catalysis 255 (2008) 48–58
JOURNAL OF CATALYSIS
www.elsevier.com/locate/jcat

Cyclopentadiene transformation over H-form zeolites: TPD and IR studies of the formation of a monomeric cyclopentenyl carbenium ion intermediate and its role in acid-catalyzed conversions

Jinlin Long, Xuxu Wang *, Zhengxin Ding, Lili Xie, Zizhong Zhang, Jingguo Dong, Huaxiang Lin, Xianzhi Fu *

Research Institute of Photocatalysis, State Key Laboratory Breeding Base of Photocatalysis, Fuzhou University, Fuzhou 350002, China

Received 14 November 2007; revised 22 January 2008; accepted 23 January 2008

Abstract

The adsorption and transformation of cyclopentadiene on HY and HZSM-5 zeolites were investigated by infrared (IR) spectroscopy and temperature-programmed desorption (TPD). The stoichiometric formation of monomeric cyclopentenyl carbenium ions ($C_5H_7^+$) was observed on the acidic sites in the supercages of zeolite HY and in the channels of zeolite HZSM-5 at room temperature, without formation of oligomerized cyclopentadiene. The IR spectra indicate that addition of quantitative cyclopentadiene led to the stoichiometric consumption of acidic OH groups. These cyclopentenyl carbocations formed in the supercages affected the vibration of the remaining OH groups at both high and low frequencies, resulting in a shift of the OH_{HF} from 3642 to 3530 cm^{-1} as well as a shift of the OH_{LF} from 3552 to 3500 cm^{-1}. The TPD-MS results reveal that the cyclopentadiene transformation on these H-form zeolites occurred at a temperature range of 473–800 K and followed a hydride ion-transfer pathway. The monomeric cyclopentenyl carbocation was the key intermediate initiating the cracking chain proceeding by the cationic mechanism.

Keywords: Infrared spectroscopy; Zeolite; Cyclopentadiene; Carbenium ion; Cracking

1. Introduction

Protonic zeolites are considered as one of the most attractive solid acid catalysts for a number of commercially important hydrocarbon transformation reactions in the petrochemical and fine chemicals industries, including olefin skeletal isomerization, alkene oligomerization, toluene disproportionation, benzene alkylation, paraffin isomerization, and cracking [1–3]. The catalytically active sites in zeolites have been not well described until now; however, the Si–OH–Al groups (i.e., Brönsted acid hydroxyl groups) in zeolites as proton donors are known to play a critical role in these hydrocarbon reactions. Numerous studies have been conducted on the adsorption and reaction of hydrocarbons on acid sites of zeolites to gain insight into the catalysis of zeolites [4–10]. It is generally accepted that the acid-catalyzed reactions of hydrocarbons on acid zeolites involve various elementary reactions, including proton addition, β-scission, oligomerization, skeletal isomerization, and hydrogen transfer, and each elementary transformation involves the formation of carbocations [11–13]. However, whether the carbocations act as transition states or as active intermediates remains under discussion [3].

Alkyl carbenium ion on zeolites has not been observed unambiguously up to now. These carbenium ions are only assumed to be formed and to act as reactive intermediates. However, several cyclic alkenyl carbenium ions, such as cyclopentenyl carbenium ions, have been found to persist in zeolites, mainly by Haw et al. using an *in situ* NMR technique [14,15]. Recently, Yang et al. also reported the formation of a few stable alkenyl carbenium ions in zeolites using *in situ* FT-IR and UV–vis spectroscopy at 150–573 K by the adsorption of cyclic precursors, including cyclopen-

* Corresponding authors. Fax: +86 591 83738606.
E-mail addresses: xwang@fzu.edu.cn (X. Wang), xzfu@fzu.edu.cn (X. Fu).

0021-9517/$ – see front matter
doi:10.1016/j.jcat.2008.01.023

tene, 1-methylcyclopentene, methylenecyclopentane, cyclohexene, and 1,3-cyclohexadiene [16]. Haw et al. proposed that these cations not only are responsible for aromatic formation and coke deposition, but also play a catalytic role in some reactions, such as MTO/MTG processes [17]. Therefore, studying the formation and transformation of cyclopentenyl carbocation is very important to gain insight into the acidity, reactivity, and deactivation of zeolites.

Cyclopentadiene as a probe reactant is theoretically a perfect precursor of the cyclopentenyl carbenium ion. However, to the best of our knowledge, the detailed intrazeolite chemistry of cyclopentadiene has not been reported to date. The main objective of the present study was to evaluate the adsorption behavior and reactivity of cyclopentadiene on H-form zeolites HY and HZSM-5 and thus attempt to gain deeper insight into the formation mechanism of cyclopentenyl carbenium ions in these zeolites.

Fourier transform infrared spectroscopy (FT-IR) is another powerful technique for studying the surface chemistry of heterogeneous catalysis [18]. It often is used to study the adsorption of olefins on H-form zeolites [19–22], because it permits direct monitoring of the interaction between hydrocarbon molecules and active sites. In the present work, we studied the detailed intrazeolite chemistry of cyclopentadiene by *in situ* FT-IR in combination with temperature-programmed desorption (TPD). We found that cyclopentadiene adsorbed on these two zeolites can be protonated to form stable cyclopentenyl carbenium ions at room temperature. These cyclopentenyl carbocations are cracked to be hydrogen acceptor products by a hydride ion-transfer mechanism under catalysis of Brönsted acid sites with increasing temperature. The acid-catalyzed transformation mechanism of cyclopentadiene in protonic zeolites is discussed.

2. Experimental

NH_4Y zeolite, with a BET surface area of ca. 700 $m^2\,g^{-1}$ and a SiO_2/Al_2O_3 ratio of 5.1 was purchased from Alfa Aesar. NH_4ZSM-5 zeolite, with a SiO_2/Al_2O_3 ratio of 50, was purchased from Zeolyst international Ltd. The materials were pressed into self-supporting IR discs (18 mm diameter, 10–20 mg) and placed into an *in situ* IR cell with CaF_2 windows, followed by thermal treatment for NH_4Y zeolite at 673 K for 20 h and for NH_4ZSM-5 zeolite at 773 K for 20 h in a flowing oxygen atmosphere. This treatment removed all nitrogen from the solid disk (as indicated by IR) without destroying the structure (as verified by XRD), and the zeolites were considered pure HY and HZSM-5 samples.

Dicyclopentadiene of >98% purity was obtained from Aldrich, with 98.6% of the dicyclopentadiene in endo form and 1.4% in exo form. Cyclopentadiene was prepared by thermal cracking and distillation of the dicyclopentadiene.

IR spectra were recorded on a Nicolet 670 FTIR spectrometer with a DTGS detector at a resolution of 4 cm^{-1}. A total of 32 scans were performed to obtain each spectrum.

TPD experiments were performed on an Autochem 2920 automatic catalyst characterization system equipped with an Omnistar GSD 30103 mass spectrograph. The sample loading was 0.2 g. The flow rate of the supporting gas (He) was 20 mL min^{-1}, and the heating rate was 5 K min^{-1}.

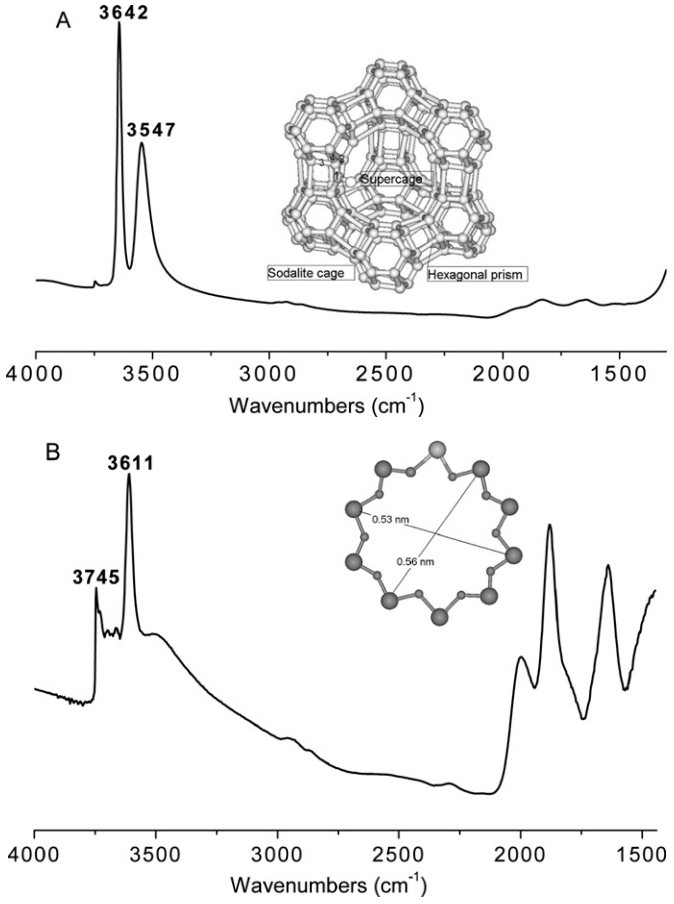

Fig. 1. (A) IR spectrum of HY zeolite and its framework structure. (B) IR spectrum of HZSM-5 zeolite and its open aperture of 10-membered ring along the [001] direction (main channel).

3. Results

3.1. Structural characteristics of HY and HZSM-5 zeolites

HY is a large-pore zeolite with a three-dimensional pore structure containing 1.25-nm-diameter supercages and 12-membered ring windows of approximately 0.75 nm. In Fig. 1A, four distinct crystallographic positions for the oxygen atoms of the framework are labeled 1–4; only the first three (O_1, O_2, and O_3) are proton positions [23]. The O_1H bond lies approximately in a plane of a 12-membered ring connecting the supercages of the structure, whereas the O_2H groups are in the plane of the six-membered ring of the sodalite units. The O_3H groups point inside the hexagonal prisms connecting the sodalite blocks [24]. After dehydration at 673 K for 3 h in vacuum, HY zeolite (ca. 13 mg disc with a diameter of 18 mm) exhibited three distinct hydroxyl bands at 3740, 3642 (high frequency [HF]), and 3547 cm^{-1} (low frequency [LF]) in the IR spectrum (Fig. 1A). Detailed data analysis reveals that the OH_{HF} band can be divided into two vibrations centered at 3642 and 3630 cm^{-1}, and that the OH_{LF} band also can be divided into three vibrations centered at 3552, 3530, and

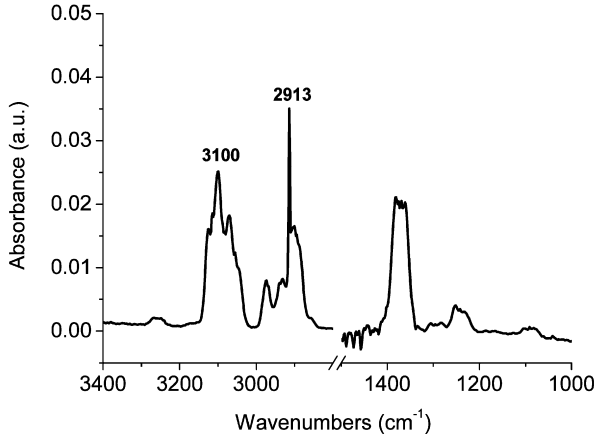

Fig. 2. FT-IR spectrum of gaseous cyclopentadiene.

3480 cm^{-1} using a Gaussian fit analysis (Fig. 3B). The bands at 3740, 3642, and 3552 cm^{-1} are assigned unambiguously to the isolated silanol groups, the acidic O_1H groups pointing inside the supercages, and the acidic O_2H groups pointing inside the sodalite cages, respectively [25]. Assignment of the 3630 cm^{-1} band remains controversial; Ward [26] ascribed it to Al–OH hydroxyl groups, but Jacobs and Uytterhoeven [27] assigned it to hydroxyls associated with aluminum-deficient sites in the zeolite lattice. We discuss this in more detail later in the paper. The band at 3530 cm^{-1} was suggested to correspond to the superacidic hydroxyls in the small cages [28]. The band at 3480 cm^{-1} is of low intensity and is very broad, and its intensity is significantly influenced by the choice of baseline. Sarria et al. [25] attributed it to the O_3H groups pointing inside the hexagonal prisms.

Unlike HY zeolite, HZSM-5 is a medium-pore zeolite that contains two intersecting channel systems. One channel is sinusoidal and runs parallel to the *a*-axis of the orthorhombic unit cell; the other channel is straight and parallel to the *b*-axis [29]. The elliptical 10-member ring openings controlling the channels have an effective diameter of ca. 0.56 nm, far smaller than that of Y zeolite. The acidic OH groups bridging to silicon and aluminum atoms in rigid crystal structures of the zeolite were observed at 3611 cm^{-1} in the IR spectrum (Fig. 1B), and the band associated with the external Si–OH groups (3745 cm^{-1}) was of modest intensity. In addition, a weaker absorption, representing mainly partially hydrolyzed framework Al (expected at around 3660–3690 cm^{-1}), was discerned between these two components.

3.2. Vibrational spectrum of gaseous cyclopentadiene

The IR spectrum of gaseous cyclopentadiene, which was in good agreement with that reported in the literature [30], is reported as a reference in Fig. 2. Five absorption bands at 3125, 3115, 3100, 3070, and 3045 cm^{-1}, assigned to =C–H stretching modes, and six bands in the region 2800–3000 cm^{-1}, assigned to $–CH_2$ stretching modes, were clearly seen. The absorptions centered at ca. 1610 and 1370 cm^{-1} can be attributed to the ν(C=C) stretching mode and the C–H deformation vibrations [δ(CH)], respectively.

3.3. IR observation of selective adsorption of cyclopentadiene on zeolite HY

Addition of a certain amount of cyclopentadiene through a syringe into the IR cell at room temperature not only decreased the OH_{HF} groups, but also affected the OH_{LF} groups, and consequently resulted in a distinct change in the IR spectrum of HY zeolite, along with a visible color change from white to red-brown. As shown in Fig. 3, in the OH-stretching region, the intensity of the 3642 cm^{-1} band, representing the acidic O_1H groups, decreased rapidly with an increasing dosage of cyclopentadiene (Fig. 3A), indicating interaction between cyclopentadiene and these OH_{HF} groups. This decrease was proportional to the amount of added cyclopentadiene (Fig. 4A). Simultaneously, the OH_{LF} band shifted slightly toward lower wavenumbers as it smoothly increased in intensity, as characterized by a positive–negative absorbance occurring in the frequency range of the LF vibrations in subtracting spectra (Fig. 3C). The same phenomenon also was observed with pyridine [31]; it indicates the presence of an interaction between cyclopentadiene and these OH_{LF} groups.

The first doses led to species characterized by bands at 1499, 1560, 1450, 2951, and 2872 cm^{-1}, which clearly differ from those of cyclopentadiene gas and cyclopentadiene adsorbed on the surface of SiO_2 (see Fig. S1 in supplementary material), as shown in Figs. 3A and 3D. The bands at 2951, 2872, and 1450 cm^{-1} corresponded to methylene ($–CH_2$)-stretching modes. In the C–H stretching region associated with sp^2-hybridized carbon, the absence of olefinic stretching modes and corresponding hydrogen-bonding band suggests that the interaction between cyclopentadiene and the acidic hydroxyls did not result in the formation of π-OH complex. After the second addition, a weak olefinic stretching mode at 3051 cm^{-1} was observed, followed by the appearance of a broad hydrogen-bonding band at ca. 3250 cm^{-1}, indicating the formation of a small amount of π-OH complex. In the 1800–1300 cm^{-1} range, three bands at 1560, 1499 and 1450 cm^{-1} became stronger. The intense band at 1499 cm^{-1} has the greatest adsorption and apparently is independent of the adsorbate, because a similar band commonly appears in the 1490–1530 cm^{-1} range on adsorption of small olefins and alcohols at 320–370 K (in some cases even at ambient temperature) [22,32–35]. Despite this, the assignment of the bands in the 1490–1530 cm^{-1} range remains under dispute, with an assignment to alkenyl carbenium ion widely accepted [20,33,36]. Compared with the carbocation spectra reported in the literature, the IR spectra of adsorbed cyclopentadiene on HY zeolite are at least consistent with a carbocation; therefore, the band at 1499 cm^{-1} can be assigned to cyclopentenyl carbenium ion species formed at room temperature. Further addition of cyclopentadiene (Fig. 4A, beyond point Q) did not provoke a change in the IR spectra, indicating that the adsorption of cyclopentadiene in the cages of HY zeolite had reached a saturated state.

The components of acid hydroxyls obtained by a Gaussian fit analysis are designated I–VII (Fig. 3B). Their frequencies are given in Table S1 (see supplementary material), and the integrated area and half bandwidth (HBW) of the different com-

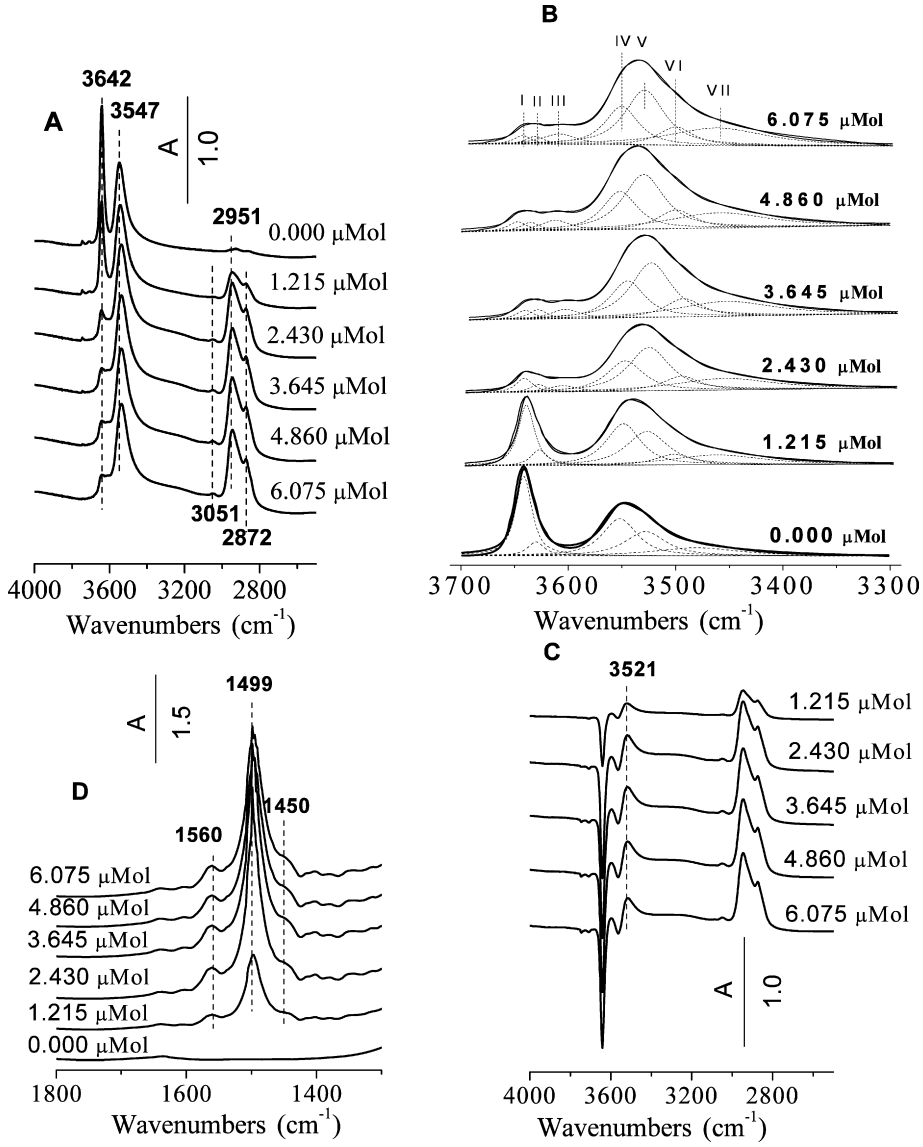

Fig. 3. (A) FT-IR spectra in the 4000–2500 cm^{-1} region of HY zeolite before and after adsorption of calculated amount of cyclopentadiene at 298 K. (B) Change in acidic hydroxyls components of HY zeolite as function of dosage amounts of cyclopentadiene. (C) Difference spectra in the 4000–2500 cm^{-1} region between HY zeolite adsorbing cyclopentadiene and HY zeolite. (D) FT-IR spectra in the 1800–1300 cm^{-1} region of HY zeolite before and after adsorption of calculated amount of cyclopentadiene at 298 K.

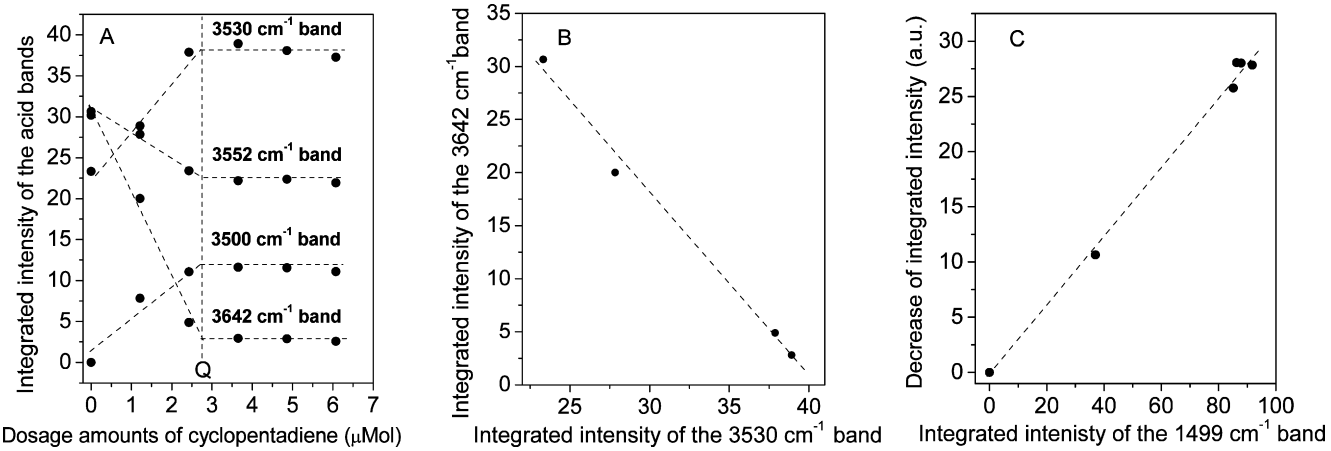

Fig. 4. (A) Change in the integrated intensity of the acidic OH band of HY zeolite with increasing the dosage amount of cyclopentadiene. (B) Correlation between the integrated intensity of the 3642 and 3530 cm^{-1} bands. (C) Correlation between the decrease of integrated intensity of the 3642 and 1499 cm^{-1} bands.

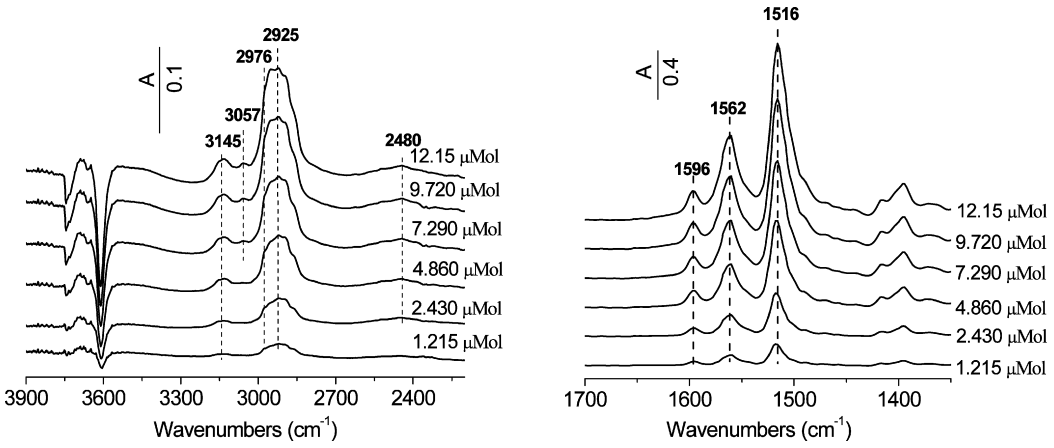

Fig. 5. FT-IR spectra of adsorption of calculated amount of cyclopentadiene on HZSM-5 zeolite at 298 K.

ponents are given in Table S2 (see supplementary material). It is interesting to note that the first doses led to a new hydroxyl component VI at ca. 3500 cm^{-1} and increased in intensity with cyclopentadiene dosage, as demonstrated by the near-linear correlation between the intensity of these OH bands and cyclopentadiene dose (Fig. 4A). The integrated intensity of the band at 3630 cm^{-1} basically represents lack of change, indicating that it is nonacidic or inaccessible. The proportional decreased integrated intensity of the bands 3642 and 3552 cm^{-1} with increasing amounts of added cyclopentadiene further confirms the interactions between cyclopentadiene and the OH_{HF} and OH_{LF} groups (Fig. 4A). More interestingly, the integrated intensity of the band at 3530 cm^{-1}, originally representing the hydroxyls in the small cages, also increased proportionally with increasing amounts of cyclopentadiene. The good linear relation between the integrated intensity of the bands at 3642 and 3530 cm^{-1} (Fig. 4B) demonstrates that this increase in intensity of the band at 3530 cm^{-1} results from the shift of the band at 3642 cm^{-1}. Thus, it can be deduced that this increased intensity of the band at 3500 cm^{-1} originates from the band at 3552 cm^{-1}, which suffers from the perturbation of protonated cyclopentadiene.

To confirm the adsorption site, we plotted the integrated intensity of the band at 1499 cm^{-1} versus the decrease of the acidic OH bands at 3642 and 3552 cm^{-1} (Fig. 4C). For the band at 3642 cm^{-1}, the good linear relation indicates that cyclopentadiene was chemically adsorbed at acidic sites in the supercages to form protonated cyclopentadiene. This can well explain the drastic decrease in intensity of the band at 3642 cm^{-1} band on dosing cyclopentadiene. The nonlinear correlation between the band at 1499 cm^{-1} and the band at 3552 cm^{-1} suggests that the interaction between cyclopentadiene and OH_{LF} groups is indirect. The OH_{LF} groups were perturbed by the protonated cyclopentadiene at the OH_{HF} sites, decreasing the intensity of the band at 3552 cm^{-1}.

3.4. IR observation of adsorption of cyclopentadiene on zeolite HZSM-5

Fig. 5 shows the IR spectra of cyclopentadiene adsorbed on HZSM-5. The band at 3611 cm^{-1}, representing the Brönsted acid hydroxyl groups of HZSM-5 zeolite, decreased in intensity

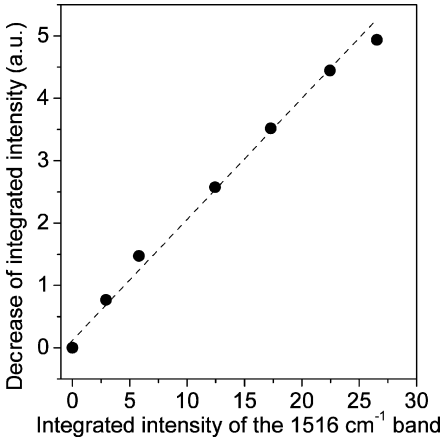

Fig. 6. Correlation between the integrated intensity of the 3611 and 1516 cm^{-1} bands.

after dosing cyclopentadiene. This indicates that the adsorption of cyclopentadiene on HZSM-5 zeolite is analogous to that on HY zeolite on Brönsted acid sites, as demonstrated by the good linear correlation between the decreased intensity of the band at 3611 cm^{-1} and cyclopentadiene dose shown in Fig. 6. With increasing amount cyclopentadiene doses, the multilayer adsorption of large amounts of cyclopentadiene occurred on the external surface of HZSM-5, as indicated by the weak band centered at 3145 cm^{-1} and the broad adsorption at ca. 2480 cm^{-1}, as well as the decrease in peak intensity of the silanol with increasing cyclopentadiene dose. The band at 3145 cm^{-1}, due to OH stretching of the bridging OHs, perturbed a medium-strong interaction with the adsorbate ($\Delta\nu = 466$ cm^{-1}). The band at 2480 cm^{-1} likely is the B component of a so-called "ABC" spectrum, due to a strong H bonding involving bridging OHs and the adsorbate [37]. This spectrum is due to the Fermi resonance of the OH stretching mode (strongly shifted downward) with the first overtones of the out of-plane bending mode of the bridging OHs [38]. Adsorption of cyclopentadiene on acidic sites inside the channels of HZSM-5 zeolite results in blockage of part of the channels and consequently hinders diffusion of the cyclopentadiene dose into the acidic sites in the inner channels. A small amount of cyclopentadiene is condensed on the external surface of HZSM-5 to form dicyclopentadiene species,

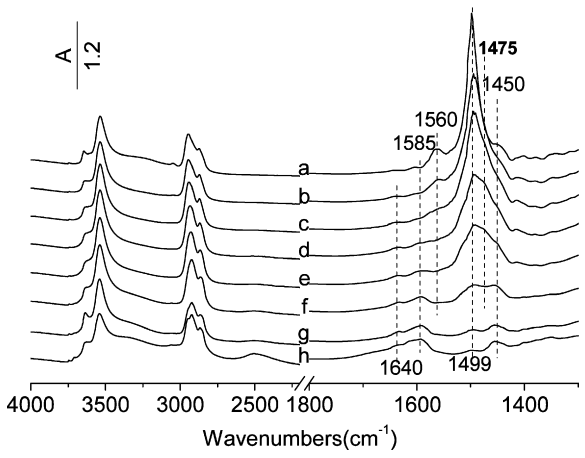

Fig. 7. FT-IR spectra of HY zeolite adsorbing cyclopentadiene upon heating at various temperatures. (a) HY zeolite adsorbing cyclopentadiene of 6.075 μmol; (b) after heating at 353 K for 0.5 h; (c) after heating at 393 K for 0.5 h; (d) after heating at 423 K for 0.5 h; (e) after heating at 443 K for 0.5 h; (f) after heating at 473 K for 0.5 h; (g) after heating at 523 K for 0.5 h; (h) after heating at 523 K for 1.5 h.

characterized by the bands at 3057, 2976, and 2925 cm^{-1}. These bands basically agree with those of cyclopentadiene adsorbed on SiO_2 shown in Fig. S1.

On adsorption of cyclopentadiene, in the 1700–1300 cm^{-1} region, several new bands could be clearly seen at 1596, 1562, and 1516 cm^{-1}. The strongest adsorption appeared at 1516 cm^{-1}, which apparently is comparable to the band at 1499 cm^{-1} in the IR spectra of HY-adsorbed cyclopentadiene. According to the literature, it also is attributed to cyclopentenyl carbenium ion species formed on the acidic sites of HZSM-5 [22,34,36]. This assignment is strongly supported by the good linear correlation between the decreased integrated intensity of the band at 3611 cm^{-1} and the integrated intensity of the band at 1516 cm^{-1} (Fig. 6). This band is 17 cm^{-1} higher than the 1499 cm^{-1} band in HY and 14 cm^{-1} lower than the sharp band at 1530 cm^{-1} in strong acidic solutions ascribed to alkenyl carbenium ions by Deno [39]. The difference between the IR absorption of cyclopentenyl carbenium ion species on HY and HZSM-5 is not well understood. It may be related to the different acidity and spatial confinement of zeolites. The bands at 1596 and 1562 cm^{-1} correspond to the C=C and C–C vibration modes, respectively, of the cyclopentenyl cation ring.

3.5. IR observation of the reactivity of cyclopentadiene over zeolites HY and HZSM-5 and regeneration of their acidic sites

Fig. 7 illustrates the drastic change in the IR spectra of cyclopentadiene adsorbed on HY with increasing reaction temperature. In the OH and CH stretching regions, the clear modifications were not detectable in the IR spectra on heating below 473 K, whereas in the CH deformation region, the characteristic absorption band of cyclopentenyl carbenium clearly decreased in intensity with increasing temperature, disappearing completely at 523 K (Fig. 7h), followed by the appearance of a coke band at 1585 cm^{-1} that cannot be completely removed under vacuum [40,41]. It also is interesting to note that a new

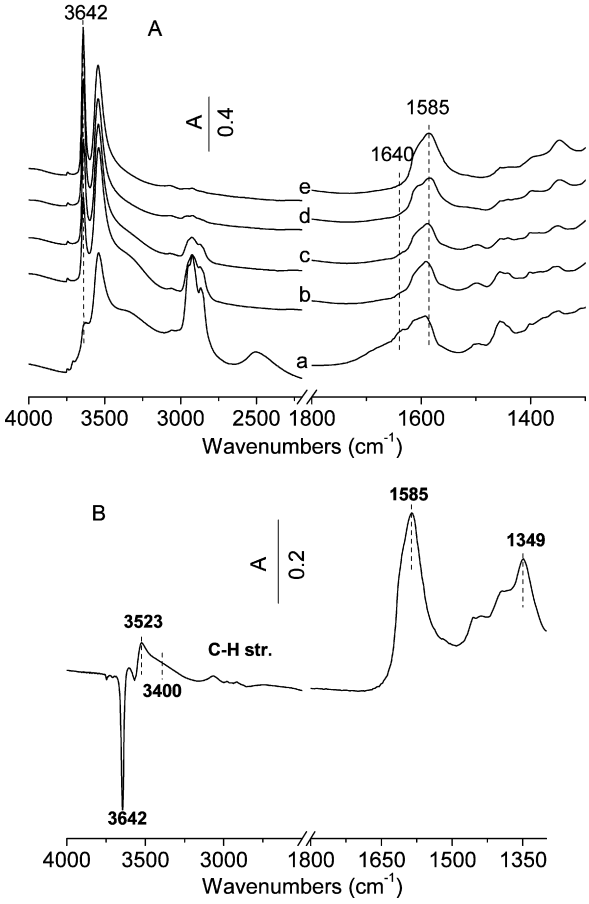

Fig. 8. (A) FT-IR spectra of HY zeolite after catalyzed-transformation of cyclopentadiene at 523 K. (a) After reaction at 523 K for 1.5 h; (b) after evacuation at 423 K for 1.0 h; (c) after evacuation at 523 K for 1.0 h; (d) after evacuation at 623 K for 1.0 h; (e) after evacuation at 673 K for 2.0 h. (B) IR of coke obtained by difference between spectra of HY zeolite before and after reaction with reaction.

band occurred at ca. 1475 cm^{-1} and increased in intensity with increasing reaction temperature from 353 to 393 K (Fig. 7, a and b). This band likely resulted from the polymerization of cyclopentenyl carbenium ions [16]. After heating at 423 K for 0.5 h, the band at 1475 cm^{-1} band in the IR spectra exhibited considerably decreased intensity, indicating cracking of these polymerized cyclopentenyl carbenium ion species at this temperature.

When the reaction temperature was increased to 523 K, a band corresponding to C=C stretching mode appeared at 1640 cm^{-1}, and the band at 1562 cm^{-1}, corresponding to the C–C bond of cyclopentenyl carbenium ion species, disappeared. This band can be removed by evacuation (Fig. 8Ab), suggesting that it belongs to the products from acid-catalyzed conversion of cyclopentenyl carbenium ions. These physisorption products on the surface of HY contained C=C bonds, demonstrating that the fraction of cyclopentadiene adsorbed over HY was transformed into other cycloalkene and alkene, as confirmed by the TPD-MS results discussed later.

After removal of physisorption species by evacuation at high temperature, most of the O_1H acidic hydroxyl groups recovered, as demonstrated by the reappearance of the IR absorption

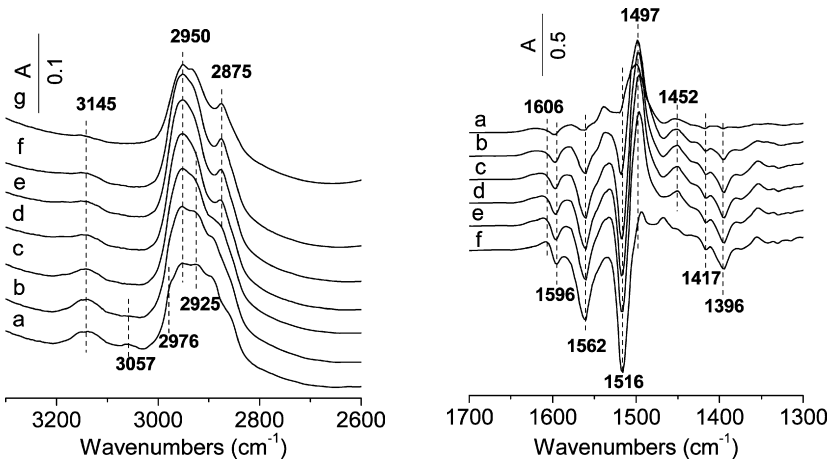

Fig. 9. FT-IR spectra of cyclopentadiene adsorbed on HZSM-5 zeolite upon heating at various temperatures. (a) After heating at 353 K for 0.5 h; (b) after heating at 393 K for 0.5 h; (c) after heating at 423 K for 0.5 h; (d) after heating at 443 K for 0.5 h; (e) after heating at 473 K for 0.5 h; (f) after heating at 523 K for 0.5 h.

band of the O_1H groups in Fig. 8A. All of these C–H stretching bands disappeared after evacuation at 673 K, whereas the coke band at 1585 cm^{-1} demonstrated no change in intensity (Fig. 8Ae). To clarify the effects of coke on the acidic hydroxyl groups, the IR spectrum of carbonaceous deposit was obtained by subtracting the IR spectrum of dehydrated HY zeolite at 673 K from Fig. 8Ae (Fig. 8B); it was found that a small amount of Brönsted acid hydroxyls in the supercages was consumed after cyclopentadiene transformation, and a corresponding hydrogen-bonding band appeared at ca. 3400 cm^{-1}. This indicates that coke was deposited on the acid sites in the supercages, resulting in the perturbation of acid hydroxyls in the supercages.

The change in the IR spectra of cyclopentadiene adsorbed on HZSM-5 zeolite with increasing reaction temperature is shown in Fig. 9. Distinct changes are apparent in the C–H stretching region; with increasing temperature, the olefinic C–H band at 3057 cm^{-1} and the bands at 2976 and 2925 cm^{-1}, corresponding to dicyclopentadiene formed on the external surface of HZSM-5, decreased in intensity along with the further decrease in intensity of the acid hydroxyl band at 3611 cm^{-1}, and disappeared at 523 K. This indicates that the dicyclopentadiene species on the external surface of HZSM-5 were diffused into channels to react with acid sites under thermal drive. More interestingly, the characteristic band of cyclopentenyl carbenium ions in the channels of HZSM-5 zeolite also shifted from 1516 to 1497 cm^{-1} on heating below 473 K. This shift toward lower wavenumbers must be related to the polymerization of cyclopentenyl carbenium ion, because no product is released below 473 K [16].

When the reaction temperature reached 523 K, most of absorption bands in the 1300–1700 cm^{-1} range decreased in intensity and some even disappeared, indicating that the transformation of the cyclopentenyl carbenium ion species formed in the channels of HZSM-5 zeolite occurred at this temperature. After evacuation under vacuum, the acid hydroxyl bands at 3611 cm^{-1} returned (Fig. 10, b and c) and a coke band was clearly visible at 1605 cm^{-1} (Fig. 10, d and e). The coke was deposited on the internal and external surface of HZMS-5.

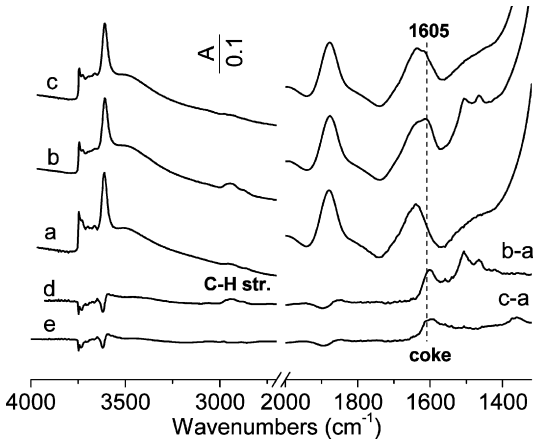

Fig. 10. FT-IR spectra of coke obtained after catalyzed-transformation of cyclopentadiene on HZSM-5 zeolite. (a) HZSM-5 zeolite dehydrated at 723 K for 3 h; (b) after catalyzed-transformation of cyclopentadiene followed by evacuation at 573 K for 1 h; (c) after evacuation at 673 K for 1 h; (d) difference between (b) and (a); (e) difference between (c) and (a).

3.6. TPD-MS study of the transformation of cyclopentadiene adsorbed on zeolites HY and HZSM-5

The results of TPD of cyclopentadiene on zeolite HY carried out under flowing He are shown in Fig. 11. The most important fragments detected between 473 and 800 K were $C_5H_9^+$ (m/z 69), C_5H_{10} (m/z 70), C_5H_8 (m/z 68), C_5H_{12} (m/z 72), C_5H_6 (m/z 66), $C_5H_7^+$ (m/z 67), $C_5H_5\cdot$ (m/z 65), $C_5H_{11}^+$ (m/z 71), $C_5H_4\cdot$ (m/z 64), C_3H_8 (m/z 44), $C_3H_7^+$ (m/z 43), C_3H_6 (m/z 42), C_4H_{10} (m/z 58), $C_4H_9^+$ (m/z 57), C_4H_8 (m/z 42), C_2H_6 (m/z 30), $C_2H_5^+$ (m/z 29), C_2H_4 (m/z 28), CH_4 (m/z 16), CH_3^+ (m/z 15), CH_2 (m/z 14), $C_{10}H_{12}$ (m/z 132), and $C_{10}H_8$ (m/z 128), with no evidence of $C_{10}H_{10}$ (m/z 130). These findings indicate that the cyclopentadiene transformation occurred in this temperature range. The TPD patterns of C_5H_{10}, $C_5H_7^+$, C_5H_8, $C_5H_9^+$, C_5H_6, $C_5H_{11}^+$, and C_5H_{12} presented a single release peak centered at ca. 553 K with a desorption onset temperature of 473 K and an amount of discharge deceasing in the order $C_5H_9^+ > C_5H_{10} > C_5H_7^+ > C_5H_8 > C_5H_{11}^+ > C_5H_6 >$

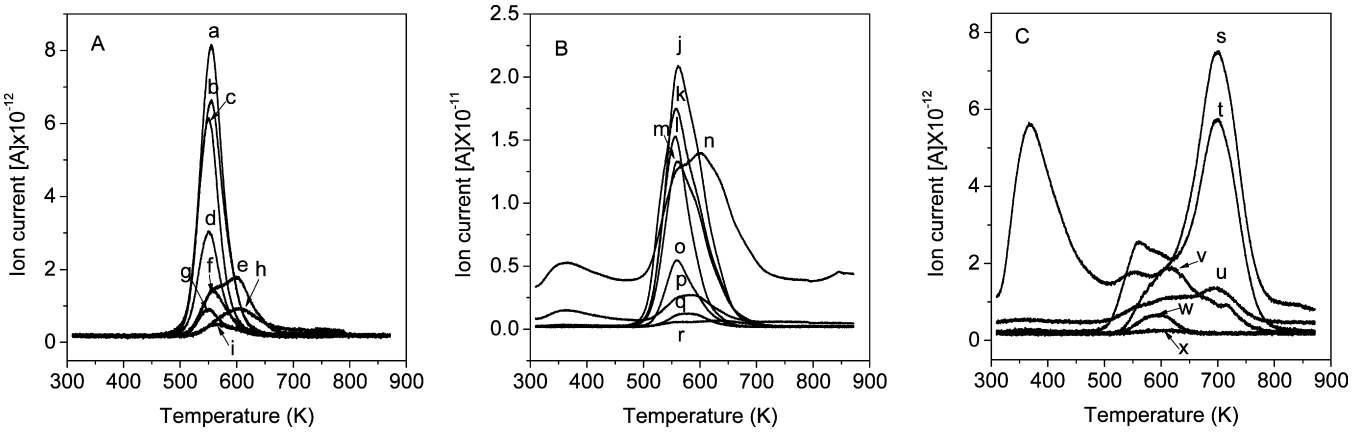

Fig. 11. TPD-MS plots of cyclopentadiene adsorbed on HY zeolite at room temperature. m/z = (a) 69; (b) 70; (c) 67; (d) 68; (e) 65; (f) 71; (g) 66; (h) 64; (i) 72; (j) 43; (k) 42; (l) 56; (m) 29; (n) 28; (o) 57; (p) 44; (q) 58; (r) 30; (s) 16; (t) 15; (u) 14; (v) 128; (x) 132.

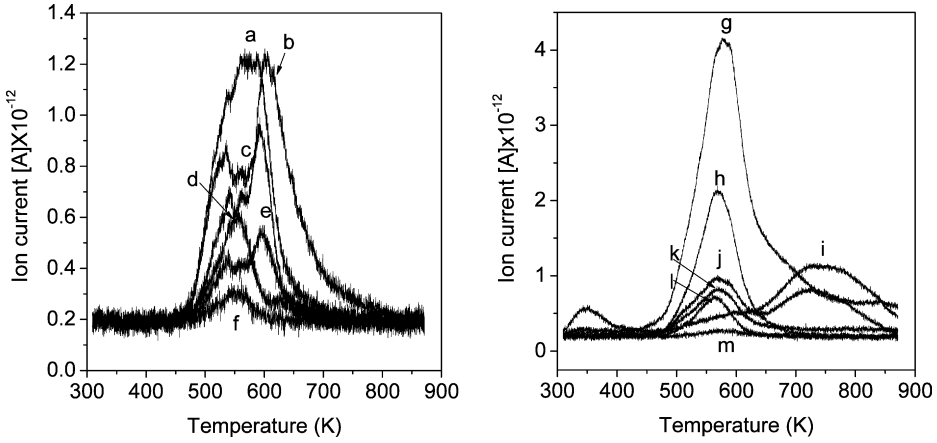

Fig. 12. TPD-MS plots of cyclopentadiene adsorbed on HZSM-5 zeolite at room temperature. m/z = (a) 65; (b) 128; (c) 132; (d) 67; (e) 130; (f) 68; (g) 28; (h) 42; (i) 16; (j) 15; (k) 44; (l) 56; (m) 30.

C_5H_{12}. This clearly indicates that cyclopentadiene adsorbed on HY was transformed into cyclopentene, cyclopentane, and pentane at 473 K. Interestingly, the large amount of discharge of $C_5H_7^+$ (m/z 67) detected at 473–623 K further confirms the IR results indicating that adsorption of cyclopentadiene at room temperature resulted in the formation of cyclopentenyl carbenium ion intermediate in the supercages of zeolite HY. As for C_3H_8, $C_3H_7^+$, C_3H_6, C_4H_{10}, $C_4H_9^+$, C_4H_8, C_2H_6, $C_2H_5^+$, and C_2H_4 organic fragments, these products from cracking reactions exhibited double release peaks at 473–800 K, whereas the C_4H_{10}, $C_4H_9^+$, and C_4H_8 fragments had a single release peak centered at 553 K. The main release peak was centered at ca. 553 K and the shoulder peak centered at ca. 600 K, where $C_3H_7^+$ (m/z 43) and C_3H_6 (m/z 44), the two main cracking products, were detected. For CH_4, CH_3^+, and CH_2 fragments, their main release peaks were centered at ca. 700 K, where CH_4 and CH_3^+ were predominant. The peak centered at 373 K was related to desorption of the physically adsorbed water.

The transformation of cyclopentadiene on HZSM-5 zeolite and the oligomerization of gaseous products occurred at 473–873 K, in basic agreement with the results obtained from the IR spectra, as demonstrated by the TPD results shown in Fig. 12. The discharges of C_3H_8 (m/z 44), C_3H_6 (m/z 42), C_4H_8 (m/z 56), C_2H_4 (m/z 28), CH_3^+ (m/z 15), CH_4 (m/z 16), $C_{10}H_8$ (m/z 128), $C_{10}H_{10}$ (m/z 130), $C_{10}H_{12}$ (m/z 132), $C_5H_7^+$ (m/z 67), C_5H_5 (m/z 65), and C_5H_8 (m/z 68), which are identical to all of the desorption products of cyclopentadiene on HY zeolite except $C_{10}H_{10}$, also were detected in this temperature range. Thus, it can be deduced that the mechanism of thermal desorption of cyclopentadiene on zeolites HZSM-5 and HY is uniform.

The overall thermal transformation processes of cyclopentadiene on H-form zeolites can be well understood by reaction equations as follows. First, cyclopentadiene is adsorbed on the acidic sites of H-form zeolites to form the cyclopentenyl carbenium ion species, which play a critical role in the transformation of cyclopentadiene into hydrogen acceptor products, such as C_5H_8, C_5H_{10}, C_5H_{12}, C_4H_{10}, C_4H_8, C_3H_8, C_3H_6, C_2H_6, C_2H_4, and CH_4 discharges. The overall reactions involve mainly carbenium ion formation, hydride ion transfer, ring opening, C–C bond scission, and oligomerization processes:

$$\text{Cyclo-}C_5H_6 + H^+ \xrightarrow{\text{Adsorption}} \text{Cyclo-}C_5H_7^+, \quad (1)$$

$$\text{Cyclo-}C_5H_7^+ + \text{Cyclo-}C_5H_6 \xrightarrow{<473\ \text{K}} \text{dienyliccation} \xrightarrow{H^+} \text{Cyclo-}C_5H_8 + \text{Cyclo-}C_5H_5^+, \quad (2)$$

$$\text{Cyclo-}C_5H_8 + H^+ \xrightarrow{\text{Adsorption}} \text{Cyclo-}C_5H_9^+, \quad (3)$$

$$\text{Cyclo-}C_5H_9^+ + \text{Cyclo-}C_5H_8 \xrightarrow{<473\ \text{K}} \text{dienyliccation} \xrightarrow{H^+} \text{Cyclo-}C_5H_{10} + \text{Cyclo-}C_5H_7^+, \quad (4)$$

$$\text{Cyclo-}C_5H_{10} + H^+ \xrightarrow{\text{Adsorption}} C_5H_{11}^+, \quad (5)$$

$$C_5H_{11}^+ + \text{Cyclo-}C_5H_{10} \xrightarrow{<473\ \text{K}} \text{dienyliccation} \xrightarrow{H^+} C_5H_{12} + \text{Cyclo-}C_5H_9^+, \quad (6)$$

$$C_5H_{12} + H^+ \rightarrow C_4H_9^+ + CH_4, \quad (7)$$

$$C_5H_{12} + H^+ \rightarrow C_4H_{10} + CH_3^+, \quad (8)$$

$$C_5H_{12} + H^+ \rightarrow C_3H_8 + C_2H_5^+, \quad (9)$$

$$C_5H_{12} + H^+ \rightarrow C_3H_7^+ + C_2H_6, \quad (10)$$

$$C_5H_7^+ \rightarrow C_5H_6 + H^+, \quad (11)$$

$$C_5H_5^+ \rightarrow C_5H_4 + H^+, \quad (12)$$

$$C_4H_9^+ \rightarrow C_4H_8 + H^+, \quad (13)$$

$$C_3H_7^+ \rightarrow C_3H_6 + H^+, \quad (14)$$

$$C_2H_5^+ \rightarrow C_2H_4 + H^+, \quad (15)$$

$$CH_3^+ \rightarrow CH_2 + H^+, \quad (16)$$

$$2C_5H_4 \rightarrow C_{10}H_8, \quad (17)$$

$$2C_5H_6 \rightarrow C_{10}H_{12}, \quad (18)$$

$$2CH_2 \rightarrow C_2H_4. \quad (19)$$

4. Discussion

4.1. Formation of monomeric cyclopentenyl carbenium ion species on H-form zeolites

Carbenium ions play a dominant role in high-temperature paraffin cracking, acting as the initiators of the cracking chain through complex ionic mechanisms. The formation and stability of such ions depend not only on the acid strength and precursors, but also on the steric constraints for protonic zeolites as a proton source [15,42]. Rosenbaum and Symons found that the capability to generate carbenium ions in sulfuric acid solution follows the order dienes > olefins > alcohols > paraffins [43]. It has been established that their formation from paraffins is difficult. Furthermore, the formation of alkyl carbenium ions through the interaction of alkenes and protons on solid acid catalysts during catalytic cracking has not been detected by IR or other spectroscopic techniques. The presence of such ions on the catalytic surface has been inferred from product distributions; however, alkenyl carbenium ions can be formed in zeolites by interaction of protons and conjugated dienes, as demonstrated by our IR spectra. The cyclopentenyl cation, a typical alkenyl carbenium ion, characterized by the band at 1499 cm^{-1} on HY and the band at 1516 cm^{-1} on HZSM-5, is particularly stable in zeolites at room temperature. It has a quite large extinction coefficient. On heating to 353 K, these two bands shifted toward lower wave numbers and then disappeared when the temperature was increased to 473–523 K. These observations are quite analogous to the IR results obtained by adsorption and reaction of 1-methylcyclopentene, cyclopentene, and 1-methylcyclopentanol on HY and HZSM-5 zeolites [16,21].

According to the Beer–Lamber law for a solution, the absorbance integrated intensity for a band is written as I: $I = \varepsilon n/S$, where ε, n, and S denote the molar extinction coefficient, number of vibrators, and area of the zeolite disc, respectively. For HY zeolite, the mean molar extinction coefficients of acid hydroxyls at high and low frequency, ε_{HF} and ε_{LF}, measured using pyridine as a probe molecule, are 7.5 and 5.6 μmol^{-1} cm, respectively [34]. Taking into account the framework Si/Al ratio of 2.55, we find that $n_{HF} = 13$ OH/u.c. and $n_{LF} = 41$ OH/u.c. Thus, in combination with the molar formula, $H_{54}(AlO_2)_{54}(SiO_2)_{138}\cdot 264H_2O$, we can deduce that the total amount of OH_{HF} groups at 3642 cm^{-1} for the HY disc of 13 mg equals 10.4 μmol. It can be seen from Fig. 3 that the two additions of cyclopentadiene led to the disappearance of ca. 84% of acidic hydroxyls at 3642 cm^{-1}; that is, ca. 8.72 μmol of acidic hydroxyls in the supercages was consumed by 2.43 μmol of cyclopentadiene. Thus, we can exclude the possibility of cyclopentenyl carbenium ions occurring in the oligomerized form. As found in a recent study of adsorption cyclopentadiene and co-adsorption of cyclopentadiene and 1-octene on cation-exchanged zeolites [44], no dicyclopentadiene species were observed when pure cyclopentadiene was contacted with the zeolites.

It has been shown that each supercage can accommodate more than four molecules of about the same kinetic diameter as pyridine [31]. From the foregoing calculated results, it is known that the ca. 13 H^+ ions per unit cell in the HY sample are located in supercages. With eight supercages per unit cell, this suggests that one cyclopentadiene molecule interacts with one OH_{HF} group, because each supercage contains ca. 1.6 OH_{HF} groups. On the basis of this assumption, the addition of 2.43 μmol cyclopentadiene will consume 2.43 μmol acidic hydroxyls to form monomeric cyclopentenyl carbenium ions. The formation of monomeric cyclopentenyl carbenium ions inevitably causes distortion of the surrounding acidic hydroxyls with a planar configuration due to the stronger electrostatic interaction and the spatial confinement, leading to a shift of most of these OHs from 3642 to 3530 cm^{-1} ($\Delta\nu = 142$ cm^{-1}). This is clearly indicated by the good linear relation between the integrated intensity of the bands at 3642 and 3530 cm^{-1} shown in Fig. 4B. These distorted OH groups can reappear at 3642 cm^{-1} on removal of these cyclopentenyl carbocations, as confirmed by the IR spectra shown in Fig. 8. Another possible cause of this disappearance is the likely transfer of protons from supercages to sodalite cages under the electrostatic interaction, as has been reported previously [45]. Therefore, theoretically, considering the different molar absorbance coefficients in the HF and LF domains, the transfer of the 6.29-μmol acidic hydroxyls to the LF domain would increase the integrated intensity of the OH_{LF} band by 13.8. This calculated value is very close to the actual increase in integrated intensity of the band at 3530 cm^{-1}

(ca. 14.5), further supporting the foregoing hypothesis. Moreover, the large amount of $C_5H_7^+$ discharge detected during the thermal desorption of cyclopentadiene adsorbed on zeolites HY and HZSM-5 provides strong evidence for monomeric adsorption. For HZSM-5, formation of the oligomerized cyclopentenyl carbenium ions is difficult, due to the spatial confinement at room temperature. Thus, it can be concluded that the cyclopentenyl carbenium ions are stably present in the monomeric form on the acidic sites of HY and HZSM-5 at room temperature.

The foregoing conclusion is reasonable from the standpoint of gas-phase proton affinity. Although 874 kJ mol^{-1} was established as the lower proton affinity limit of compounds that can be expected to be fully protonated by a zeolite [46,47], some less basic compounds, such as hexamethylbenzene (PA = 860.6 kJ mol^{-1}) and 1,2,4,5-tetraMB (durene) (PA = 818 kJ mol^{-1}), can be protonated to carbenium ions [42,48]. Cyclopentadiene has a PA value of ca. 825.0 kJ mol^{-1} [49], slightly more basic than that of durene, and thus it also can be protonated to a stable cyclopentenyl carbenium ion, such a durene, in a zeolite.

However, heating the monomeric cyclopentenyl carbenium ions at 353–423 K caused them to polymerize to dienylic or trienylic carbenium ions, as indicated by the shifts of the characteristic band from 1499 to 1475 cm^{-1} in HY zeolite and from 1516 to 1497 cm^{-1} in HZSM-5 zeolite. These results are similar to those of Xu and Haw [15], who detected the formation of trimerized cyclopentenyl carbenium ions at 323–393 K by adsorption of cyclopentenol on HY zeolite using *in situ* NMR.

To further confirm our findings, we used cyclopentadiene dimer as a precursor and evaluated its adsorption on zeolite HY by FTIR spectroscopy. Interestingly, the IR spectra (see Fig. S2 in supplementary material) were quite similar to those shown in Fig. 3 and very different than those of dicyclopentadiene adsorbed on silicon [50]. This indicates that the same adsorbed species are formed in zeolites using these two precursors, originating mainly from the conversion of dicyclopentadiene to cyclopentadiene.

4.2. Transformation of cyclopentenyl carbenium ions

In the temperature range 473–673 K, the main desorption products of cyclopentadiene on zeolites HY and HZSM-5 were alkanes, alkenes, cyclo-alkane, cyclo-alkenes, and alkenyl carbenium ions. In addition, a small amount of cyclopentadiene dimer was produced. These are basically identical to the findings reported by Anderson et al. [51]. However, a key question that we must consider is derived from these hydrogen acceptor products: Where are the extra hydrogens without introducing the outer hydrogen? The precise answer to this question involves the cracking processes of hydrocarbons using zeolites, which in genera, can be classified according to three main mechanistic pathways: type I, a classical cracking mechanism comprising a hydride-transfer step to a carbenium ion followed by β-scission; type II, a nonclassical Haag–Dessau (protolytic) cracking mechanism proceeding via a carbenium ion transition state; and type III, oligomerization cracking [3]. In our case, the transformation of cyclopentadiene on zeolites HY and HZSM-5 proceeded in two steps via the classical cracking mechanism consisting of cyclopentenyl carbenium ion formation and hydride ion transfer. This pathway is based on carbocation chemistry, as demonstrated by Eqs. (1)–(19) in Section 3.6. It provides a relatively comprehensive description of the cyclopentadiene transformation and can account for all important desorption products and the recovery of most of the acid hydroxyls.

All of the conversions from C_5H_6 to C_5H_8, from C_5H_8 to C_5H_{10}, and from C_5H_{10} to C_5H_{12} need to undergo a protonation, polymerization, and hydride ion-transfer process according to the aforementioned pathway. The hydride ion transfer also includes a hydride ion-transfer reaction from C_5H_{12} to a surface carbenium ion that results in an alkane product and a smaller carbenium ion. The latter cation deprotonates or desorbs as C_2, C_3, and C_4 olefins or participates in other reactions. Thus, the hydride ion cycles yield both paraffins and olefins. But the further isomerization of cracking products possibly proceeds in parallel with these cracking reactions. In addition, the conversion from C_5H_8 to C_5H_{10} also possibly contains a contribution from disproportionation of cyclopentene, which is thermodynamically favorable at this temperature range [51]. These possibilities cannot be completely excluded from the TPD-MS results. The reaction of cyclopentadiene with Brönsted acid sites of HY and HZSM-5 zeolites is accompanied by coke formation along with the foregoing reaction scheme, as demonstrated by the coke IR band in Figs. 8 and 10. The coke deposition, formed on these two zeolites during the transformation of cyclopentenyl carbocations, offers a clue as to the source of additional hydrogen atoms. It is very likely that these extra hydrogens are derived from the transformation of some of the cyclopentenyl carbocations in dienylic or trienylic form to polyaromatic species containing much less hydrogen via such processes as dehydrogenation, polymerization, and so on.

5. Conclusion

In this work, we investigated the adsorption and transformation of cyclopentadiene on zeolites HY and HZSM-5 by *in situ* IR spectroscopy and TPD and found that cyclopentadiene could be adsorbed on the acidic sites inside the supercages of zeolite HY and the acidic sites of zeolite HZSM-5 to form monomeric cyclopentenyl carbenium ions at room temperature. The addition of quantitative cyclopentadiene led to the stoichiometric consumption of acidic OH groups. These cyclopentenyl carbocations formed in the supercages affected the vibration of the remaining OH groups in both high and low frequencies, resulting in a shift of the OH_{HF} from 3642 to 3530 cm^{-1} and a shift of the OH_{LF} from 3552 to 3500 cm^{-1}. IR spectra indicate that the monomeric cyclopentenyl carbocation likely was oligomerized to di-enylic or tri-enylic carbenium ions at 353–423 K and then transformed to alkanes and alkenes on heating above 473 K. Deposition of small amounts of coke in the supercages or channels led to a decrease in acidic hydroxyls and restoration of most of the acidic sites. TPD-MS findings show

that the cyclopentadiene transformation on these H-form zeolites followed a hydride ion-transfer pathway.

Acknowledgments

This work was supported by the National Natural Science Foundation of China (grants nos. 20673020 and 20537010) and the National Basic Research Program of China (973 Program, no. 2007CB613306).

Supplementary material

The online version of this article contains additional supplementary material.

Please visit DOI: 10.1016/j.jcat.2008.01.023.

References

[1] H. García, H.D. Roth, Chem. Rev. 102 (2002) 3947.
[2] A. Corma, Chem. Rev. 95 (1995) 559.
[3] M. Stöcker, Microporous Mesoporous Mater. 82 (2005) 257.
[4] J.N. Kondo, K. Domen, J. Mol. Catal. A Chem. 199 (2003) 27.
[5] E. Yoda, J.N. Kondo, K. Domen, J. Phys. Chem. B 109 (2005) 1464.
[6] A. Chica, K. Strohmaier, E. Iglesia, Langmuir 20 (2004) 10982.
[7] A. Trombetta, A.G. Alejandre, J.R. Solis, G. Busca, Appl. Catal. A Gen. 198 (2000) 81.
[8] T. Armaroli, M. Bevilacqua, M. Trombetta, A.G. Alejandre, J.R. Solis, G. Busca, Appl. Catal. A Gen. 220 (2001) 181.
[9] S. Kotrel, M.P. Rosynek, J.H. Lunsford, J. Phys. Chem. B 103 (1999) 818.
[10] L. Song, Z. Sun, L. Duan, J. Gui, G.S. McDougall, Microporous Mesoporous Mater. 104 (2007) 115.
[11] G. Yaluris, R.J. Madon, J.A. Dumesic, J. Catal. 165 (1997) 205.
[12] J. Sommer, D. Habermacher, M. Hachoumy, R. Jost, A. Reynaud, Appl. Catal. A Gen. 146 (1996) 193.
[13] M. Guisnet, N.S. Gnep, Appl. Catal. A Gen. 146 (1996) 33.
[14] J.F. Haw, B.R. Richadson, I.S. Oshiro, N.D. Lazo, A.J. Speed, J. Am. Chem. Soc. 111 (1989) 2052.
[15] T. Xu, J.F. Haw, J. Am. Chem. Soc. 116 (1994) 7753.
[16] S. Yang, J.N. Kondo, K. Domen, Catal. Today 73 (2002) 113.
[17] J.F. Haw, J.B. Nicholas, W. Song, F. Deng, Z. Wang, T. Xu, C.S. Heneghan, J. Am. Chem. Soc. 122 (2000) 4763.
[18] J. Ryczkowski, Catal. Today 68 (2001) 263.
[19] F. Geobaldo, G. Spoto, S. Bordiga, C. Lamberti, A. Zecchina, J. Chem. Soc. Faraday Trans. 93 (1997) 1243.
[20] M. Bjørgen, K.P. Lillerud, U. Olsbye, S. Bordiga, A. Zecchina, J. Phys. Chem. B 108 (2004) 7862.
[21] J.N. Kondo, H. Ishikawa, E. Yoda, F. Wakabayashi, K. Domen, J. Phys. Chem. B 103 (1999) 8538.
[22] S. Yang, J.N. Kondo, K. Domen, J. Phys. Chem. B 105 (2001) 7878.
[23] M. Csjzek, H. Jobic, A.N. Fitch, T. Vogt, J. Phys. Chem. 96 (1992) 1535.
[24] K.S. Smirnov, J. Phys. Chem. B 105 (2001) 7405.
[25] F.R. Sarria, O. Marie, J. Saussey, M. Daturi, J. Phys. Chem. B 109 (2005) 1660.
[26] J.W. Ward, Adv. Chem. 101 (1971) 380.
[27] P.A. Jacobs, J.B. Uytterhoeven, J. Chem. Soc. Faraday Trans. 1 69 (1973) 359.
[28] A. Chambellan, T. Chevreau, S. Khabtou, M. Marzin, J.C. Lavalley, Zeolites 10 (1992) 306.
[29] G.T. Kokotailo, S.L. Lawton, D.H. Olson, W.M. Meier, Nature 272 (1978) 437.
[30] E. Gallinella, B. Fortunato, P. Mirone, J. Mol. Spectrosc. 24 (1967) 345.
[31] S. Khabtou, T. Chevreau, J.C. Lavalley, Microporous Mater. 3 (1994) 133.
[32] J.F. Joly, N. Zanier-Szydlowski, S. Colin, F. Raatz, J. Saussey, J.C. Lavalley, Catal. Today 9 (1991) 31.
[33] S. Jolly, J. Saussey, J.C. Lavalley, J. Mol. Catal. 86 (1994) 401.
[34] S. Yang, J.N. Kondo, K. Domen, Stud. Surf. Sci. Catal. 135 (2001) 217.
[35] H. Lechert, C. Dimitrov, C. Bezouhanova, V. Nenova, J. Catal. 80 (1983) 457.
[36] I. Kirisci, H. Förster, G. Tasi, J.B. Nagy, Chem. Rev. 99 (1999) 2085.
[37] A. Gutiérrez-Aljejandre, M.A. Larrubia, J. Ramirez, G. Busca, Vib. Spectrosc. 41 (2006) 42.
[38] A.G. Pelmenschikov, R.A. van Stanten, J. Phys. Chem. 97 (1993) 10678.
[39] N.C. Deno, in: G.A. Olah, R.P. Schleyer (Eds.), Carbonium Ions, vol. II, Wiley, New York, 1970, p. 783.
[40] G. Caeiro, J.M. Lopes, P. Magnoux, P. Ayrault, F. Ramôa-Ribeiro, J. Catal. 249 (2007) 232.
[41] B. Paweewan, P.J. Barrie, L.F. Gladden, Appl. Catal. A Gen. 185 (1999) 259.
[42] M. Bjørgen, F. Bonino, S. Kolboe, K.P. Lillerud, A. Zecchina, S. Bordiga, J. Am. Chem. Soc. 125 (2003) 15863.
[43] J. Rosenbaum, M.C.R. Symons, J. Chem. Soc. (1961) 1.
[44] J.F.M. Denayer, A. Depla, W. Vermandel, F. Gemoets, F.V. Buren, J. Martens, C. Kirschhock, G.V. Baron, P.A. Jacobs, Microporous Mesoporous Mater. 103 (2007) 1.
[45] T.R. Hughes, H.M. White, J. Phys. Chem. 71 (1967) 2192.
[46] J.B. Nicholas, J.F. Haw, J. Am. Chem. Soc. 120 (1998) 11804.
[47] J.F. Haw, Phys. Chem. Chem. Phys. 4 (2002) 5431.
[48] M. Bjørgen, F. Bonino, B. Arstad, S. Kolboe, K.P. Lillerud, A. Zecchina, S. Bordiga, ChemPhysChem 6 (2005) 232.
[49] G. Bouchoux, J.Y. Salpin, Chem. Phys. Lett. 366 (2002) 510.
[50] G.T. Wang, C. Mui, C.B. Musgrave, S.F. Bent, J. Phys. Chem. B 103 (1999) 6803.
[51] J.R. Anderson, Y.F. Chang, R.J. Western, J. Catal. 118 (1989) 466.